TRANSNAV the International Journal on Marine Navigation and Safety of Sea Transportation
http://www.transnav.eu
Volume 15
Number 2
June 2021
DOI: 10.12716/1001.15.02.04

# Influence of Mutual Position of Communication Network Users on Accuracy of Positioning by Telemetry Method

M. Džunda & P. Dzurovčin
*Technical University of Kosice, Kosice, Slovakia*

ABSTRACT: In this paper we solve the problem of the influence of the mutual position of the users of the communication network on the accuracy of the telemetric navigation system. We present the principle of operation of a telemetry navigation system and examine the accuracy of determining the position of users of the communication network depending on their mutual position. The telemetric method of determining the position of users of a communication network can be used in shipping or air transport. The simulation of the telemetry system will be performed in the Matlab software environment.

## 1 INTRODUCTION

Air transport is one of the regular modes of transport and it is therefore essential that it be as safe as possible. The intensive development of aviation, which occurred after the Second World War, led to an increase in capacity and a reduction in air traffic. At the same time, this caused an increase in more frequent collisions of aircraft in the air. For this reason, it was necessary to develop a system that would increase air safety and help prevent such collisions. Several types of anti-collision systems have been developed in the history of aviation. Significant progress in their development did not come until 1981. At this time, the currently best-known active on-board anti-collision system TCAS (*Traffic Alert and Collision Avoidance System*) was improved. The development of this system continues today even today due to the ever-increasing demands on air safety. TCAS means additional safety insurance in air traffic. There are also financially and technically less demanding anti-collision systems, such as the PCAS system, the so-called mobile anti-collision system. Thanks to its specific properties, this passive system is also suitable for its installation in smaller aircraft and, due to its financial availability, it is intended mainly for the needs of general aviation. Anti-collision systems are currently a key element in increasing the level of air safety. In our research we have devoted the alternative possibility of determining the position of aircraft without the use of satellite navigation systems, based on the principles of relative navigation (RelNav). In order for this method of navigation to be applicable, it is necessary to analyze the accuracy of the system and its application within the concept of the future communication and navigation infrastructure. The main goal of the paper is to evaluate the accuracy of position determination by the RelNav system depending on the position of users of the communication network. Work related to relative navigation is focused on research in formation flights, in-flight refueling and initial navigation, which is directly dependent on GNSS. Currently, relative navigation is most important for mapping and navigating UAV resources in a GNSS-free environment. We published the results of the evaluation of the accuracy of the relative navigation system in [2–4]. The results of the simulation of the

RelNav system presented in these works confirm that the accuracy of this system deteriorates as the distance between the users of the communication network increases. We have also found that the accuracy of the RelNav system depends on the relative position of the users of the communication network. The [6] work presents a method improve DME distance measuring accuracy by using a new DME pulse shape. The proposed pulse shape was developed by using Genetic Algorithms and is less susceptible to multipath effects so that the ranging error reduces by 36.0–77.3% when compared to the Gaussian and Smoothed Concave Polygon DME pulses, depending on noise environment. The [5] paper introduces optimal ground station augmentation algorithms that help to efficiently transform the current DME ground network to enable a DME/DME positioning accuracy of up to 0.3 nm or 92.6 m with a minimal number of new ground DME sites. The positioning performance and augmented ground network using the proposed Stretched-Front-Leg (SFOL) pulse-based DME are evaluated in two regions which have distinct terrain conditions. The [10] Distance Measuring Equipment (DME) is seeing renewed interest for its ability to support future aviation navigation and surveillance needs. It is one of the major technologies being examined by the FAA Alternative Position Navigation and Timing (APNT) program to support needs to provide an alternative to GNSS in a NextGen airspace. Facility data-base resolution and fidelity, and precision of DME ground system location surveys are a function of today's 0.2 nm system error limit. These errors become noticeable when viewing flight data that is processed to the tighter tolerances required by APNT. Their contribution to system error will likely require reduction [1]. The navigation subsystem in most platforms is based on an inertial navigation system (INS). Regardless of the INS grade, its navigation solution drifts in time. To avoid such a drift, the INS is fused with external sensor measurements such as a global navigation satellite system (GNSS). In situations when maneuvering helps to improve state observability, virtual lever-arm (VLA) measurements manage to gain additional improvement in accuracy. These results are supported by simulation and field experiments with a vehicle mounted with a GNSS and an INS [8]. Positioning accuracy of area navigation (RNAV) is directly related to geometric dilution of precision (GDOP). For the distribution of three DME beacons, this paper establishes the GDOP algorithm model based on DME/DME RNAV, the GDOP calculation is deduced, and the relation between GDOP and DME ground station distribution is given. The affection of the geometric configuration and the baseline length of DME stations, and of the aircraft height on GDOP values are studied and simulated by MATLAB. In [7] the optimal methods of DME beacon distribution for DME/DME RNAV are proposed and all these results will provide theoretical guidance for implementation of DME/DME RNAV in China. Alternative positioning navigation by DME service network is used in many cases on-board of aircraft. This problem is topical in case of bad accuracy of GNNS, spatially during takeoff or landing phases of aircraft flight. In the paper, an accurate approach of positioning by data from DME with support of all available DMEs signals in particular point of airspace has been discussed. An availability area of Ukrainian DME service network for altitude of FL320 has been evaluated. Dilution of precision coefficient for geometrical factor estimation in accuracy calculation of positioning by DME network for Ukrainian airspace was used [13]. A typical type of a DME pulse being used in practice is a Gaussian pulse, and the achievable DME ranging accuracy is primarily determined by the pulse shape. [Kim, E. 2013] presents an alternative DME pulse waveform that is able to provide much higher range accuracy than the conventional Gaussian pulse. The alternative pulse waveform is compliant with the pulse shape requirements in the current DME specifications to maintain the compatibility with existing DME ground transponders and avionics. In addition, the paper discuss the potential constraints in implementing the alternative pulse in the existing transponders and avionics. The Multi-constellation Global Navigation Satellite System (Multi-GNSS) has become the standard implementation of high accuracy positioning and navigation applications. It is well known that the noise of code and phase measurements depend on GNSS constellation. Then, Helmert variance component estimation (HVCE) is usually used to adjust the contributions of different GNSS constellations by determining their individual variances of unit weight. However, HVCE requires a heavy computation load [12]. [Zhao, J. et. Aall 2018] presents a new method to improve the accuracy in the heading angle estimate provided by low-cost magnetometers on board of small Unmanned Aerial Vehicles (UAVs). This task can be achieved by estimating the systematic error produced by the magnetic fields generated by onboard electric equipment. The magnetic biases' determination problem can be formulated as a system of non-linear equations by exploiting the acquired visual and GNSS data [19]. The Chinese Area Positioning System (CAPS) is a new positioning system developed by the Chinese Academy of Sciences based on the communication satellites in geosynchronous orbit. The CAPS has been regarded as a pilot system to test the new technology for the design, construction and update of the BeiDou Navigation Satellite System (BDS). BDS-3 type is equipped with two major functions, namely navigation and positioning, as well as data communication. BDS can provide seven types of services. The results indicate a potential application of CAPS for highly accurate positioning and speed estimation and the availability of a new navigation mode based on communication satellites [16]. At the same time, many applications do not require precise absolute Earth coordinates, but instead, inferring the geometric configuration information of the constituent nodes in the system by relative positioning. The Real-Time Kinematic (RTK) technique shows its efficiency and accuracy in calculating the relative position. The efficiency test shows that the proposed method can be a real-time method, the time that calculates one epoch of measurement data is no more than 80 ms and is less than 10 ms for best results. The novel method can be used as a more robust and accurate ambiguity free tracking approach for outdoor applications [15]. To bridge the GPS outage for multicopters is designed proposes a novel navigation reconstruction method for small multicopters, which combines the vehicle dynamic model and micro-electro-mechanical system

(MEMS) sensors. Firstly, an induced drag model is introduced into the dynamic model of the vehicle, and an efficient online parameter identification method is designed to estimate the model parameters quickly. In addition, the nongravitational acceleration estimated from body velocity and radar height are utilized to yield a more accurate attitude estimate. Some types of Multi-Static Surveillance Radars are described in [17-18]. Fusing the information of the attitude, body velocity, magnetic heading, and radar height, a navigation system based on an error-state Kalman filter is reconstructed. Simulation results show that the proposed navigation reconstruction algorithm aided by the vehicle model can significantly improve navigation accuracy during a GPS outage [14]. This article demonstrates the superiority of a fuzzy tracking system over the standard Kalman filter tracking system under the conditions of uneven accelerations and sudden change of direction of the targets, as well as in the case of failure to observe the target during successive scans. A cascading Kalman filtering algorithm was used to solve the speed ambiguity and to reduce the measurement error in real-time radar processing. The cascade filters are extended Kalman filters with controlled gain using fuzzy logic for tracking targets using radar equipment under difficult tracking conditions [11]. An automatic landing of an unmanned aerial vehicle (UAV) is a non-trivial task requiring a solution of a variety of technical and computational problems. The most important is the precise determination of altitude, especially at the final stage of approaching to the earth. With current altimeters, the magnitude of measurement errors at the final phase of the descent may be unacceptably high for constructing an algorithm for controlling the landing manoeuvre. One of the possible and straightforward ways is the camera resolution change by pixels averaging in computer part which performed in coordination with theoretically estimated and measured OF velocity. The article presents results of such algorithms testing from real video sequences obtained in flights with different approaches to the runway with simultaneous recording of telemetry and video data [9]. Over the past years Time-of-Flight (ToF) sensors have become a considerable alternative to conventional distance sensing techniques like laser scanners or image based stereo-vision. Due to the ability to provide full-range distance information at high frame-rates, ToF sensors achieve a significant impact onto current research areas like online object recognition, collision prevention or scene and object reconstruction. The main contribution, in this context, is a new intensity-based calibration model that requires less input data compared to other models and thus significantly contributes to the reduction of calibration data.

## 2 POSITIONING BY TELEMETRY METHOD

The principle of the telemetric method is described in detail in [4]. Next, in accordance with [4], we will state algorithms for calculating the flying object position. Telemetry is the automatic measurement and wireless transmission of data from remote sources. The location of the FO is determined by acquiring the transmissions from three (or more) different locations to triangulate the location of the device. Each user in communication network transmits a signal which contains information about its position and the current time at regular intervals. These signals, travelling at the speed of light, are intercepted by a receiver of an unknown user, which calculates how far each user is based and how long it takes for the signal to arrive. The range from the other users is determined by the time the signal is received. To ensure the work of the RelNav system, at least three users must be visible to the unknown receiver at all times. The location of the unknown user is calculated by the following solution system of three equations [4]:

$$\sqrt{(x_i - x)^2 + (y_i - y)^2 + (z_i - z)^2} = d_i \tag{1}$$

where: $x_i$, $y_i$, $z_i$- geocentric coordination of the user, di – range between an unknown receiver and each transmitter, x, y, z- geocentric coordination of an unknown receiver.

The distances to the users are derived from the transmitted signals and they are affected by uncertainties in clock setting, therefore they are normally referred to as pseudo-ranges. There is a time synchronization problem of each user´s clock. The Pseudo-range measurements lead to a pseudo-ranging four point problem which is the problem of determining the four unknowns. The unknowns comprise the three components of the receiver position {X, Y, Z} and the stationary receiver range bias. Four pseudo-range equations are expressed algebraically as [4]:

$$(x - x_1)^2 + (y - y_1)^2 + (z - z_1)^2 - (b - d_1)^2 = 0 \tag{2}$$

$$(x - x_2)^2 + (y - y_2)^2 + (z - z_2)^2 - (b - d_2)^2 = 0 \tag{3}$$

$$(x - x_3)^2 + (y - y_3)^2 + (z - z_3)^2 - (b - d_3)^2 = 0 \tag{4}$$

$$(x - x_4)^2 + (y - y_4)^2 + (z - z_4)^2 - (b - d_4)^2 = 0 \tag{5}$$

where: $d_1$, $d_2$, $d_3$, $d_4$ – measured pseudo-distances from a source of transmission to receivers, $x_{1\text{-}4}$, $y_{1\text{-}4}$, $z_{1\text{-}4}$ – coordinates of users, x, y, z- coordinates of the receiver, b – shift of the time basis of the receiver converted into distance.

For subtraction (5) from (2), is valid:

$$f_{14} = x_{14}x + y_{14}y + z_{14}z + d_{41}b + e_{14} \tag{6}$$

For subtraction (5) from (3), is valid it holds:

$$f_{24} = x_{24}x + y_{24}y + z_{24}z + d_{42}b + e_{24} \tag{7}$$

For subtraction (5) from (4), is valid:

$$f_{34} = x_{34}x + y_{34}y + z_{34}z + d_{43}b + e_{34} \tag{8}$$

If variable b is considered as constant (the so-called factor of homogenization), then, depending on expressions (6-8), a system of three equations with three unknown variables is obtained. We have applied the method of resultants of the multi-polynomials to solve the system of linear equations *x=g(b), y=g(b), z=g(b)* [4].

Following is valid:

$$f_1 = \left(x_{14}x + d_{41}b + e_{14}\right)k + y_{14}y + z_{14}z \tag{9}$$

$$f_2 = \left(x_{24}x + d_{42}b + e_{24}\right)k + y_{24}y + z_{24}z \tag{10}$$

$$f_3 = \left(x_{34}x + d_{43}b + e_{34}\right)k + y_{34}y + z_{34}z \tag{11}$$

If the variable "k" turns into the factor of homogenization, Jacobi's determinant of the coordinate *x* by (9), (10), (11) is expressed as:

$$J_x = det\begin{pmatrix} \frac{df_1}{dy} & \frac{df_1}{dz} & \frac{df_1}{dk} \\ \frac{df_2}{dy} & \frac{df_2}{dz} & \frac{df_2}{dk} \\ \frac{df_3}{dy} & \frac{df_3}{dz} & \frac{df_3}{dk} \end{pmatrix} = \det \tag{12}$$

In compliance with (9-11), for *y = g (b)* is valid:

$$f_4 = \left(y_{14}y + d_{41}b + e_{14}\right)k + x_{14}x + z_{14}z \tag{13}$$

$$f_5 = \left(y_{24}y + d_{42}b + e_{24}\right)k + x_{24}x + z_{24}z \tag{14}$$

$$f_6 = \left(y_{34}y + d_{43}b + e_{34}\right)k + x_{34}x + z_{34}z \tag{15}$$

Jacobi's determinant for the coordinate *y* is expressed as:

$$J_y = det\begin{pmatrix} \frac{df_4}{dx} & \frac{df_4}{dz} & \frac{df_4}{dk} \\ \frac{df_5}{dx} & \frac{df_5}{dz} & \frac{df_5}{dk} \\ \frac{df_6}{dx} & \frac{df_6}{dz} & \frac{df_6}{dk} \end{pmatrix} = det \tag{16}$$

In compliance with (9-11), for *z = g (b)* is valid:

$$f_7 = \left(z_{14}z + d_{41}b + e_{14}\right)k + x_{14}x + y_{14}y \tag{17}$$

$$f_8 = \left(z_{24}z + d_{42}b + e_{24}\right)k + x_{24}x + y_{24}y \tag{18}$$

$$f_9 = \left(z_{34}z + d_{43}b + e_{34}\right)k + x_{34}x + y_{34}y \tag{19}$$

Jacobi´s determinant for coordinate *z* is expressed as:

$$J_z = det\begin{pmatrix} \frac{df_7}{dx} & \frac{df_7}{dy} & \frac{df_7}{dk} \\ \frac{df_8}{dx} & \frac{df_8}{dy} & \frac{df_8}{dk} \\ \frac{df_9}{dx} & \frac{df_9}{dy} & \frac{df_9}{dk} \end{pmatrix} = det \tag{20}$$

From expressions (12), (16), (20) we obtain the value of the determinants $J_x$, $J_y$, $J_z$. We get the variable equations *x=g(b), y=g(b), z=g(b)* by applying the value of each determinant. Substituting the expression for x, y, z into the equation (2), the quadratic function for the unknown variable b is obtained:

$$Ab^2 + Bb^2 + C = 0 \tag{21}$$

Solutions of the quadratic equation (21) have two roots, b+ and b-. Therefore we have to calculate the coordinates of the FO (x+, y+, z+) and P (x-, y-, z-). To come to the correct solution, we have to calculate the norm ( $norm = \sqrt{x^2 + y^2 + z^2}$ ) for (x, y, z) b- and (x, y, z) b+. If the coordinates of the receiver are fed into the coordinate reference system, the norm of the position vector will be close to the value of the radius of the Earth (Re = 6372.797 km) and this solution for the FO (x, y, z) will be regarded as a correct one [4].

### 2.1 *Evaluation of the influence of users location on the accuracy of the RelNav system*

In accordance with algorithms 1 to 21, we performed evaluation of the influence of users location on the accuracy of the RelNav system. Using simulation, we investigate the effect of the geometric distribution of flying objects on the accuracy of determining their position. The test cases are designed to examine the sensitivity of the relative navigation system to this factor.The simulation results are shown in figure 1 to 5.

In our simulation, we assume that LOT5MF is a flying object whose position we want to determine. We know the coordinates FO RJA39K, FHM6112, LOT653 and WZZ3007. It is clear from the theory of navigation that the accuracy of determining the position of the FO rangefinder method depends on the accuracy of measuring the distance from own rangefinders to the rangefinders of the others systems and on the geometry of the rangefinder systems. Therefore, we checked how the accuracy of the RelNav system will depend on the FO geometries working in the aviation communication network. We performed further simulations and investigated the accuracy of FO positioning when changing the geometry of communication network users. The simulations were performed for a straight flight lasting 1375 s. When selecting the geometry of users of the aviation communication network, we proceeded as follows. We will consider FO LOT5MF as an unknown FO. The initial positions of the LO in the simulation for a distance of 5 km are shown in Figure no. 1 and in table no. 1 and 2. When selecting the initial coordinates of the network users, we placed the individual users with respect to the geographical course of the LOT5MF flight. The geographical course

of the LOT5MF flight will be 345° for all simulations. The geographic course of the initial position of the user of the RJA39K communication network will be 48°. The geographic course of the initial position of the user of the communication network FHM6112 will be 19°. The geographic rate of the initial position of the user of the LOT653 communication network will be 318°. The geographic course of the initial position of the user of the communication network WZZ3007 will be 286°. In the individual simulations, we gradually changed the distances between LOT5MF and users RJA39K, FHM6112, LOT653 and WZZ3007 in the range of 5 to 50 km. The initial positions of the LO in the simulation for a distance of 5 km are shown in Figure no. 1 and in table no. 1 and 2.

Table 1. Initial LO coordinates in the WGS-84 system and in the coordinate system ECEF, distance 5 km

| FO | identification | latitude (°) | longitude (°) |
|---|---|---|---|
| 1. | RJA39K | 48.8022 | 21.1971 |
| 2. | FHM612 | 48.8143 | 21.1657 |
| 3. | LOT653 | 48.8080 | 21.1097 |
| 4. | WZZ3007 | 48.7856 | 21.0838 |
| 5. | LOT5MF | 48.771 | 21.148 |

| | latitude (rad) | longitude (rad) | height above sea level |
|---|---|---|---|
| 1. | 0.851759 | 0.369959 | 11262 |
| 2. | 0.851970 | 0.369411 | 10683 |
| 3. | 0.851860 | 0.368433 | 7003 |
| 4. | 0.851469 | 0.367982 | 10363 |
| 5. | 0.851215 | 0.369102 | 3784 |

| | X (km) | Y (km) | Z (km) |
|---|---|---|---|
| 1. | 3931.154 | 1524.565 | 4784.573 |
| 2. | 3930.688 | 1521.907 | 4785.025 |
| 3. | 3930.405 | 1517.382 | 4781.793 |
| 4. | 3934.907 | 1517.076 | 4782.678 |
| 5. | 3930.301 | 1520.361 | 4776.659 |

Picture no. 1 shows the distribution of FO1-4 users with respect to FO5 for a distance of 5 km. The initial coordinates of the FO are marked with a black (+) sign, which indicates the identification mark of the individual FO.

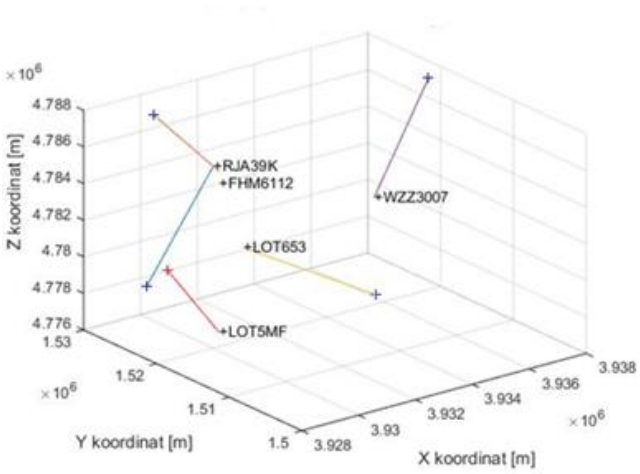


Figure 1. Flight trajectories of five FO, straight flight, shift 5 km, flight length 1375 s.

The results of the FO positioning simulation are shown in FIG. 2 to 5. In FIG. no. 2 shows the errors of measuring the distance Δd1 to Δd4 between LOT5MF and other network users as a function of time. From picture no. 2 shows that the mean values of the distance measurement errors Δd1 to Δd4 range from -0.03 m to 0.02 m and the dispersions of the distance measurement errors Δd1 to Δd4 range from 0.98 m² to 1.01 m².

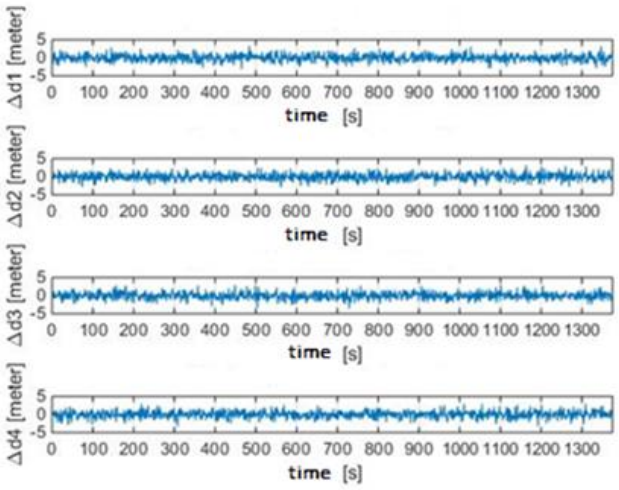


Figure 2. Errors in measuring the distance Δd1 to Δd4 between LOT5MF and other network users.

In FIG. no. 3 shows the error of determining the coordinates ΔX, ΔY, ΔZ and the error of determining the position FO5 ΔP as a function of time. From picture no. 3 shows that the mean values of the coordinate errors ΔX, ΔY, ΔZ range from - 0.03 m to 0.06 m and the dispersion of coordinate errors ΔX, ΔY, ΔZ ranges from 2.81 m2 to 9.80 m2. The mean value of the positioning error FO 5 mΔP is equal to 3.84 m and the dispersion of the positioning error FO 5◎2ΔP is equal to 6.04 m2.

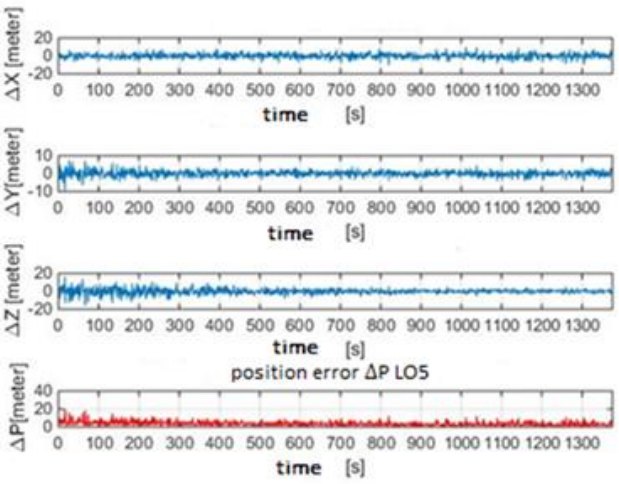


Figure 3. Coordinate determination errors ΔX, ΔY, ΔZ and position error ΔP FO5, rectilinear flight 1375 s

In picture no. 4 is a histogram of the positioning error LO 5. It can be seen from the figure that the maximum number of positioning errors is in the range of 0.8 to 7.64 m.

In order to verify the sensitivity of the derived algorithm to the accuracy of FO 5 positioning, which works in the aviation communication network, we performed additional simulations. We maintained the initial coordinates of FO RJA39K, FHM6112, LOT653 and WZZ3007 in the above courses and changed their

distances from LOT5MF in the range of 10 to 50 km. The results of the simulation when changing the distances of FO 5 from other FO 1 to 4 from 5 to 50 km are shown in Figure no. 5. From picture no. 5 shows that the mean value of the positioning error FO 5 $m_{\Delta P}$ was in the range of 3.5 to 10.0 m and the dispersion of the positioning error FO 5 $\sigma^2_{\Delta P}$ varied in the range of 7.0 to 72.79 $m^2$. From picture no. 5 shows that as the distances FO RJA39K, FHM6112, LOT653 and WZZ3007 from LOT5MF increase, the positioning errors increase. Based on this, we can conclude that the accuracy of determining the position of a flying object operating in the aviation communication network depends on the mutual position of network users. Our proposed RelNav system is accurate. The subject of further research will be the dependence of the accuracy of this system on the mutual position of the users of the communication network. vv

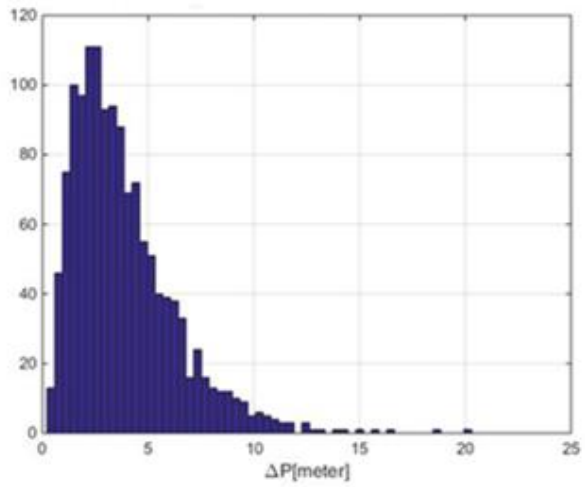


Figure 4. FO5 positioning error histogram

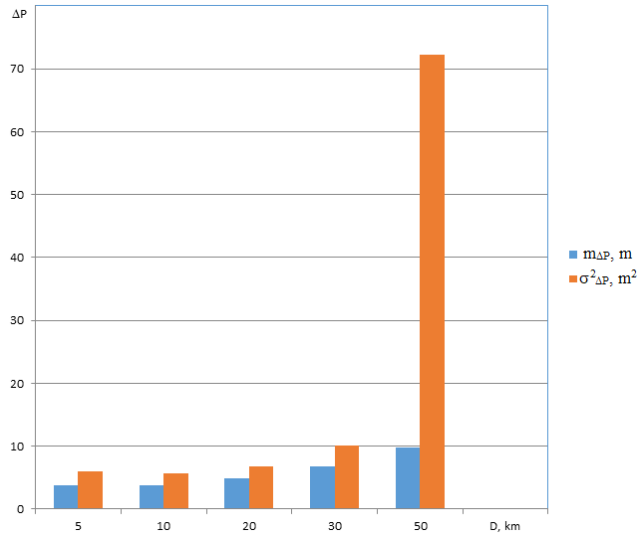


Figure 5. LO 5 positioning accuracy for straight flight and distances from 5 to 50 km.

## 3 CONCLUSION

Using derived algorithms and a model of the motion of flying objects, we performed a computer simulation, which is used to determine the position of the unknown LO 5 and evaluate the accuracy of the proposed system RelNav. The computer simulation was performed in the Matlab programming environment and explains the principle of operation of the RelNav system. The result of modeling is a total of five models that simulate the motion of LO in a geocentric coordinate system. A description of the models is given in [4]. LO motion models represent input data for computer simulation. In order for the simulation to correspond to reality as much as possible, we performed observations of air traffic over the territory of the Slovak Republic via the Flightradar24 application. We randomly selected five FOs, whose geographical coordinates and heights we implemented in our model. For the needs of solving the problem, it was necessary to transform the coordinates into a geocentric coordinate system. The result of the simulation is the evaluation of the accuracy of determining the position of FO 5 for different model situations. The simulation results confirmed that the accuracy of FO position determination in the RelNav system depends on the geometry of the communication network users. The principles of relative navigation can also be applied to maritime 2D navigation. The basic condition for the correct operation of such a system in the navy is to create a communication network of users and to ensure time synchronization of data transmission by individual users. We assume that for the accuracy of determining the location of the user of this network will be the same as for the aviation communication network. In further research, it would be appropriate to verify the navigation possibilities of flying and floating objects (ships) in the relative navigation system.

## REFERENCES


1. Borko, A., Klein, I., Even-Tzur, G.: GNSS/INS Fusion with Virtual Lever-Arm Measurements. Sensors. 18, 7, (2018). https://doi.org/10.3390/s18072228.
2. Džunda, M., Dzurovčin, P., Melniková, L.: Determination of Flying Objects Position. TransNav, the International Journal on Marine Navigation and Safety of Sea Transportation. 13, 2, 423–428 (2019). https://doi.org/10.12716/1001.13.02.21.
3. Džunda, M., Kotianová, N.: Presnosť relatívnej navigácie v komunikačnej sieti letectva. TU, Košice (2017).
4. Džunda, M., Kotianová, N., Dzurovčin, P., Szabo, S., Jenčová, E., Vajdová, I., Koščák, P., Liptáková, D., Hanák, P.: Selected Aspects of Using the Telemetry Method in Synthesis of RelNav System for Air Traffic Control. International Journal of Environmental Research and Public Health. 17, 1, (2020). https://doi.org/10.3390/ijerph17010213.
5. Kim, E.: Alternative DME/N pulse shape for APNT. In: 2013 IEEE/AIAA 32nd Digital Avionics Systems Conference (DASC). pp. 4D2-1 (2013). https://doi.org/10.1109/DASC.2013.6712591.
6. Kim, E., Seo, J.: SFOL Pulse: A High Accuracy DME Pulse for Alternative Aircraft Position and Navigation. Sensors. 17, 10, (2017). https://doi.org/10.3390/s17102183.
7. Li, M., Nie, W., Xu, T., Rovira-Garcia, A., Fang, Z., Xu, G.: Helmert Variance Component Estimation for Multi-GNSS Relative Positioning. Sensors. 20, 3, (2020). https://doi.org/10.3390/s20030669.
8. Li, S., Ni, Y., Cai, N.: Optimal strategy of DME beacon distrbution for DME/DME area navigation. In: 2012 IEEE 11th International Conference on Signal

Processing. pp. 2036–2039 (2012). https://doi.org/10.1109/ICoSP.2012.6491981.
9. Lindner, M., Schiller, I., Kolb, A., Koch, R.: Time-of-Flight sensor calibration for accurate range sensing. Computer Vision and Image Understanding. 114, 12, 1318–1328 (2010). https://doi.org/10.1016/j.cviu.2009.11.002.
10. Lo, S., Chen, Y.H., Enge, P., Peterson, B., Erikson, R., Lilley, R.: Distance Measuring Equipment Accuracy Performance Today and for Future Alternative Position Navigation and Timing (APNT). Presented at the Proceedings of the 26th International Technical Meeting of the Satellite Division of The Institute of Navigation (ION GNSS+ 2013) September 20 (2013).
11. Miller, A., Miller, B., Popov, A., Stepanyan, K.: UAV Landing Based on the Optical Flow Videonavigation. Sensors. 19, 6, (2019). https://doi.org/10.3390/s19061351.
12. Opromolla, R.: Magnetometer Calibration for Small Unmanned Aerial Vehicles Using Cooperative Flight Data. Sensors. 20, 2, (2020). https://doi.org/10.3390/s20020538.
13. Ostroumov, I.V., Kuzmenko, N.S.: Accuracy estimation of alternative positioning in navigation. In: 2016 4th International Conference on Methods and Systems of Navigation and Motion Control (MSNMC). pp. 291–294 (2016). https://doi.org/10.1109/MSNMC.2016.7783164.
14. Raboaca, M.S., Dumitrescu, C., Manta, I.: Aircraft Trajectory Tracking Using Radar Equipment with Fuzzy Logic Algorithm. Mathematics. 8, 2, (2020). https://doi.org/10.3390/math8020207.
15. Xu, Y., Zhang, Q., Zhang, J., Wang, X., Yu, Z.: A Vehicle-Model-Aided Navigation Reconstruction Method for a Multicopter during a GPS Outage. Electronics. 10, 5, (2021). https://doi.org/10.3390/electronics10050528.
16. Yang, W., Liu, Y., Liu, F.: An Improved Relative GNSS Tracking Method Utilizing Single Frequency Receivers. Sensors. 20, 15, (2020). https://doi.org/10.3390/s20154073.
17. Zacik, N., Holoda, S., Novak, A., Otto, I., Jonas, P.: *Multi-Static Surveillance Radar Primary Data Simulation*. Belgrade: City Net Scien Res Ctr Ltd-Belgrade, 2018, pp. 1–6.
18. Zacik, N., Novak, A.: *Passive Radar System for Slovakia*. : Scientific Research Center Ltd Belgrade, 2016, pp. 31–35.
19. Zhao, J., Li, Z., Ge, J., Wang, L., Wang, N., Zhou, K., Yuan, H.: The First Result of Relative Positioning and Velocity Estimation Based on CAPS. Sensors. 18, 5, (2018). https://doi.org/10.3390/s18051528.